



ISSN:2229-6107



**INTERNATIONAL JOURNAL OF
PURE AND APPLIED SCIENCE & TECHNOLOGY**

**E-mail :
editor.ijpast@gmail.com
editor@ijpast.in**

www.ijpast.in

New Power Balancing According to Standard 1459

M GIRIBABU¹ , L.M.L. NARAYANA REDDY²

Abstract—

Numerous investigations in active power compensators used to enhance power network quality have been prompted by the growing concern about harmonic distortion and load unbalances in recent years. In this study, we provide a novel method for resolving the unbalanced power that is analogous to the method employed in IEEE Std. 1459 for the non-fundamental effective apparent power. When shunt active power compensators are installed at customer premises to enhance power quality, the recommended power magnitudes provide for an explanation of the outcomes attained. In this study, we offer new merit factors related to the new imbalance power resolution to quantify the quality of the setup. The resolution is used to assess both simulated and experimental outcomes in the study.

Key words

Active power filters, electrical power-quality indexes, IEEE Std. 1459, revenue power amounts, unbalanced power resolution are all terms that may be found in an index.

Introduction

Increases in energy consumption are a concern for governments and energy providers in our increasingly industrialized and modern world [1, 2, 3, 4]. Rising fossil fuel costs, caused in part by rising global demand for electricity, have sparked widespread interest in harnessing renewable energy sources like wind and solar [1, 2]. Engineers striving for peak electrical system efficiency also face serious challenges from poor power quality [5–13]. Different lenses are used to the study of electrical power quality issues. Definitions of electrical power [5, 6], definitions of electric power-quality indexes [14, 16], evaluations of electric energy quality [18–21], electrical energy billing [22–24], identification and localization of inefficient loads [21], and active compensators [5–9] are just a few of the more recent topics being

researched and developed. The updated definitions for measuring electric power in sinusoidal, non-sinusoidal, balanced, and unbalanced situations may be found in IEEE Standard 1459 [16]. IEEE Std. 1459 is meant to be used in the assessment of cutting-edge apparatus or in the development of next-generation instruments for measuring power and energy [16, 25]. While [25]–[27] provide various analyses and explanations of IEEE Std. 1459 terminology, [14] formulates several IEEE Std. 1459 words using an instantaneous power method. Instrumentation that meets the requirements of IEEE Std. 1459-2000 is shown in [28] through [30]. At its heart, each of these gadgets has a Digital Signal Processor (DSP) that runs complex algorithms on data gathered from the instrument's measurement of line-to-neutral and

Assistant professor^{1,2}

DEPARTMENT OF ELECTRICAL AND ELECTRONICS ENGINEERING
P.B.R.VISVODAYA INSTITUTE OF TECHNOLOGY & SCIENCE
S.P.S.R NELLORE DIST, A.P , INDIA , KAVALI-524201

three-phase load voltages and currents [30]. According to IEEE Std. 1459, the updated definitions were created to aid in the measurement and monitoring of revenue-relevant quantities [22]–[24], engineering economic choices, and the identification of important harmonic polluters [19–21], [31], [32]. Government rules in certain countries and electrical utility tariffs [22], [24] determine the cost for the various power levels. According to [21], identifying who is responsible for the presence of certain power amounts, whether it be end users or electrical utilities, is essential for accurate electrical energy invoicing. The necessity for new indices "for the evaluation of harmonic distortion levels at the metering section and for the determination of loads and supply polluting contributions" is also emphasized. The "Toll Road" model of [20] and [31] aims to assign and allocate the cost and expenditures of the circuits required to maintain the power network with the least possible harmonic pollution. Quality issues arise in electrical power networks when loads necessitating basic positive-sequence reactive power, unbalance power, and non-fundamental effective apparent power are present [9], [10]. Historically, banks of capacitors have been used to compensate for reactive power [5, 19]. Passive and active compensators, as well as hybrid configurations, are used to reduce unbalanced power and harmonic distortion [5, 33, 34]. In low-voltage distribution networks, shunt active compensators are favoured at the terminal non-linear load that requires harmonic currents [5, 9, 33].

NUMBERING TO IEEE STANDARD 1459

According to IEEE Std. 1459, the following are the primary electrical quantities for three-phase power systems. Included in the total measure of "fundamental powers" provided by "fundamental effective apparent power" are, among others, and. Whole-load apparent power generated by the flow of harmonic components of the load current and the PCC voltage is quantified by the non-fundamental powers, which are represented as. The effective apparent power, as described by the standard, is the product of the effective voltage and current. In contrast to the other powers (, and), which are not related to the efficient transmission of energy from generators to loads, is regarded a useful power quantity [6, 16], [25], [28]. In contrast to the more popular "non active powers," which include include active basic negative-sequence power and active fundamental zero-sequence power, as well as harmonic active power, the phrase "useless powers" is favoured. Unlike in IEEE Std. 1459, where

resolution is not done, the PCC voltages and load currents are resolved as shown in (1).

$$S_{eN}^2 = D_{eI}^2 + D_{eV}^2 + S_{eH}^2.$$

The power magnitudes that appear in (1) are as follows.

- The current distortion power . It is calculated from the product of the fundamental effective voltage and the harmonic effective current , as it appears in (2). quantifies the part of produced by the current distortion. This is usually the dominant component of S_{eN}

$$D_{eI} = 3I_{eH}V_{e1}.$$

- The voltage distortion power . It is calculated in (3) from the product of the fundamental effective current. and the harmonic effective voltage . quantifies the part of produced by the voltage distortion.

$$D_{eV} = 3I_{e1}V_{eH}.$$

The harmonic apparent power . It is calculated in (4) from the product of the effective harmonic current and the effective harmonic voltage . quantifies the part of produced by the product of voltage and current harmonic components

$$S_{eH} = 3I_{eH}V_{eH}.$$

Unbalance Power decomposition

The unbalance power quantifies the effect of the load fundamental current unbalances jointed with the PCC fundamental voltage asymmetries. is a fundamental power that is calculated from the resolution of ? can be expressed as a function of and or as the quadratic sum of all the fundamental power quantities as follows:

$$(S_{e1})^2 = (3V_{e1}I_{e1})^2 = (P_1^+)^2 + (Q_1^+)^2 + (S_{U1})^2.$$

The value of is calculated from (10) as follows

$$\begin{aligned} (S_{U1})^2 &= (S_{e1})^2 - (P_1^+)^2 - (Q_1^+)^2 \\ &= (S_{e1})^2 - (S_1^+)^2 \end{aligned}$$

where is the effective apparent power of the basic positive sequence? In [14], the basic symmetrical

components of the PCC voltages and line currents are used to do the computation. An ideal balanced resistive load will need a number of unbalanced currents if the PCC basic voltages are not perfectly symmetrical. Following IEEE Std. 1459, a SAPC's primary function is to transform the customer load into a balanced resistive load that only requires [6, 16], [25], and [28] in order to operate. It is difficult to achieve this target if PCC fundamental voltages exhibit asymmetries, as the customer is not responsible for all of the unbalanced power. The SAPC can only decrease specific powers due to basic voltage anomalies at the PCC. This was found for the first time in the course of evaluating the simulation results and experimental data reported in [6]. The SAPC implemented in [6] supplies the load current components associated with the presence of, and. To minimize the high-frequency harmonic content introduced by the VSI inverter's self-switching operation, the SAPC is able to produce a balanced set of supply fundamental currents. The client needs just the "on" or "active" portion of the basic "positive-sequence current," which is the only component of the current that is directly connected to the existence of. Some electrical words associated with and maintained in the supply lines as part of regular SAPC functioning. Since the SAPC cancels properly, both and are zero, but the converse is not true. Since the PCC has voltage asymmetries and harmonic voltage distortion, a SAPC will not be able to totally nullify the wasteful energies. If is employed in this instance to impose a penalty, the customer will be forced to foot the bill for an issue that originated in the electrical grid.

PREDICTED OUTCOMES

The proposed decomposition (, and) and the updated merit factors (and) are verified using some simulated outcomes. The averaged model of the circuit shown in Fig. 3 uses the values ;. The inductances for the ac output are offered for choosing in [35]. In [6], you can read more about the simulation model and the control algorithm used in SAPC. Figure 4 depicts the simulation results for the PCC line to neutral voltages, which have fundamental voltage asymmetries with rms values of 220 V, 230 V, and 205 V, respectively. The frequency at its core is 50 hertz. A balanced linear load with the following parameters is utilized as the simulation load. The neutral current (lower plot) and load currents (upper plot) are shown in Fig. 5. Because of the asymmetry in the PCC voltage, the load currents are not balanced, and the rms neutral current is 2.18 A. The data in Tables I and II

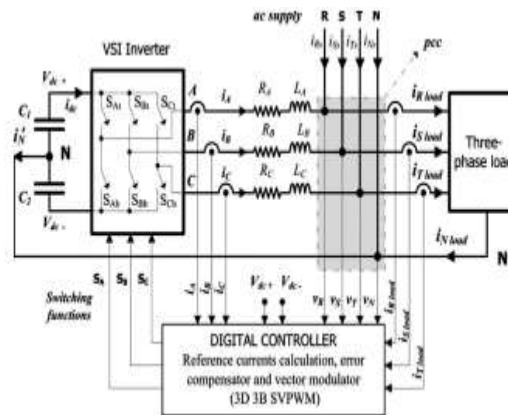


Fig. 1. SAPC connection to the power network.

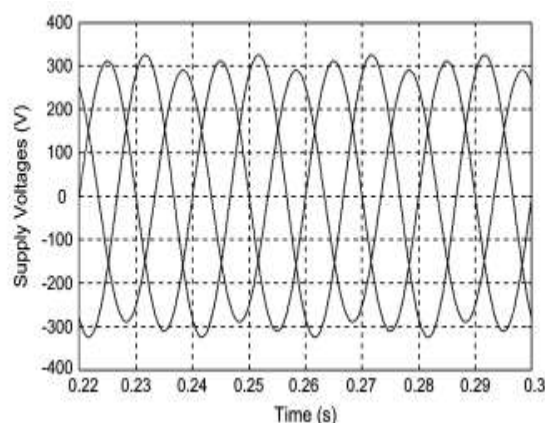


Fig. 2. Phase-to-neutral voltages used in the simulations

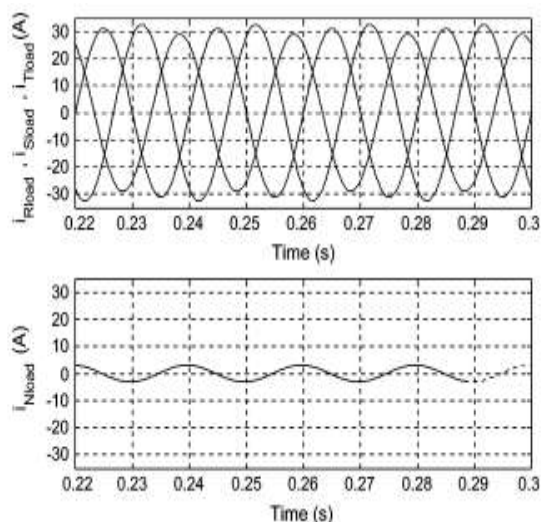


Fig. 3. Phase (top) and neutral (bottom) currents for a pure resistive three-phase balanced load.

the main magnitudes of the circuit. Table I includes the voltages, currents, power magnitudes, and merit factors of the three-phase balanced linear load. The values included in the tables are grouped according to the magnitudes represented:

- Voltages V_e , V_{e1} , V_1^+ , V_{eH} , and V_{eU} are calculated from the rms line to neutral voltages ($V_R - V_S - V_T$).

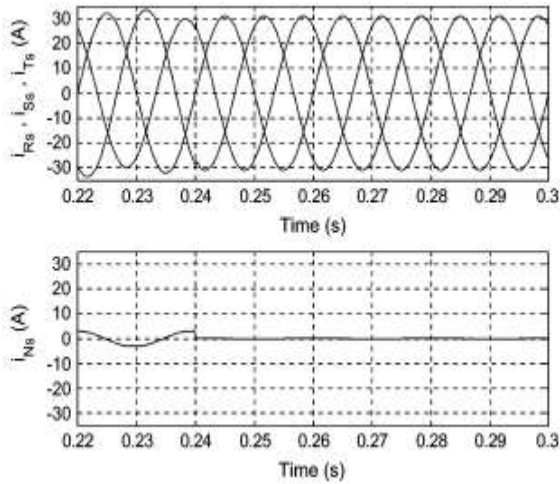


Fig. 4. Phase (top) and neutral (bottom) supply currents after SAPC operation.

TABLE I LOAD VOLTAGE, CURRENT, AND POWER MAGNITUDES DURING THE SIMULATION

$V_R = 220$ V	$V_S = 230$ V	$V_T = 205$ V
$V_e = 218.51$ V	$V_{e1} = 218.51$ V	$V_{eH} = 0$ V
$V_1^+ = 218.33$ V	$V_1^- = 7.25$ V	$V_1^0 = 7.27$ V
$V_{eU} = 8.89$ V	$V_1^-/V_1^+ = 3.32$ %	$V_1^0/V_1^+ = 3.33$ %
$I_{R1} = 22$ A	$I_{S1} = 23$ A	$I_{T1} = 20.5$ A
$I_{N1} = 2.18$ A		
$I_e = 21.87$ A	$I_{e1} = 21.87$ A	$I_{eH} = 0$ A
$I_1^+ = 21.81$ A	$I_1^- = 0.72$ A	$I_1^0 = 0.72$ A
$I_{eU} = 1.62$ A	$I_1^-/I_1^+ = 3.32$ %	$I_1^0/I_1^+ = 3.33$ %
$S_e = 14337.86$ VA	$S_{e1} = 14337.86$ VA	$S_{eH} = 0$ VA
$S_1^+ = 14286.40$ VA	$P_1^+ = 14286.40$ W	$Q_1^+ = 0$ var
$P_1 = 14318.10$ W	$P = 14318.10$ W	$S_{U1} = 1212.56$ VA
$P_R - P_{R1} = 4830.53$ W	$P_S - P_{S1} = 5287.26$ W	$P_T - P_{T1} = 4200.31$ W
$P_F = P_{F1} = 0.9986$		$P_{F1}^+ = 1$
$S_{UV} = 583.31$ VA	$S_{U1} = 1063.91$ VA	$S_{U1U} = 43.28$ VA
$P_1^- = 15.77$ W	$P_1^0 = 15.83$ W	$S_{U1e} = 29.58$ VA
$TU_V = 4.07$ %		$TU_I = 7.42$ %

- Currents I_e , I_{e1} , I_1^+ , I_{eH} , and I_{eU} are calculated from the rms line supply currents and the rms current through the neutral wire

EXPERIMENTAL RESULTS

To verify the validity of the proposed power quantities and factors, some experimental results are obtained with the smallscale prototype described in [6]. The experimental test reproduces different supply conditions and load values than in the simulations, to increase the effect of the load unbalances and voltage asymmetries.

$$S_{eN}, D_{eI}, D_{eV}, S_{eH}, \text{ and } P_H$$

exist in the experimental test. The SAPC operates reducing all the exiting useless load powers as is described in [6]. The load used in the test is implemented using an unbalanced linear load in parallel with a balanced three-phase non-linear load. Fig. 8 shows the load current waveforms, and the rms values of the load currents are detailed on the right of the scope. The waveforms are captured with a Yokogawa DL7100 oscilloscope. The scale used in all oscilloscope current waveforms is

$$100 \text{ mV} \equiv 1 \text{ A} .$$

The per-phase non-linear load is built using a

TABLE II EXPERIMENTAL LOAD VOLTAGE, CURRENT, AND POWER MAGNITUDES

$V_R = 124.24$ V	$V_S = 123.82$ V	$V_T = 78.71$ V
$V_e = 110.50$ V	$V_{e1} = 110.48$ V	$V_{eH} = 2.10$ V
$V_1^+ = 108.89$ V	$V_1^- = 15.52$ V	$V_1^0 = 14.68$ V
$V_{eU} = 18.68$ V	$V_1^-/V_1^+ = 14.26$ %	$V_1^0/V_1^+ = 13.48$ %
$I_{R1} = 6.02$ A	$I_{S1} = 4.59$ A	$I_{T1} = 1.75$ A
$I_{N1} = 5.80$ A		
$I_e = 5.60$ A	$I_{e1} = 4.83$ A	$I_{eH} = 2.82$ A
$I_1^+ = 3.78$ A	$I_1^- = 1.24$ A	$I_1^0 = 1.37$ A
$I_{eU} = 3.01$ A	$I_1^-/I_1^+ = 32.85$ %	$I_1^0/I_1^+ = 36.30$ %
$THD_{I_e} = 29.43$ %	$THD_{I_{e1}} = 41.23$ %	$THD_{I_{eH}} = 85.36$ %
$S_e = 1884.70$ VA	$S_{e1} = 1601.17$ VA	$S_{eH} = 936.04$ VA
$S_1^+ = 1234.15$ VA	$P_1^+ = 1205.09$ W	$Q_1^+ = 266.24$ var
$P_1 = 1315.01$ W	$P = 1324.13$ W	$S_{U1} = 1020.10$ VA
$P_R = 701.56$ W	$P_S = 521.55$ W	$P_T = 101.02$ W
$P_{R1} = 698.90$ W	$P_{S1} = 516.81$ W	$P_{T1} = 99.30$ W
$P_F = 0.7139$	$P_{F1} = 0.8213$	$P_{F1}^+ = 0.9764$
$S_{UV} = 270.68$ VA	$S_{U1} = 997.90$ VA	$S_{U1U} = 168.70$ VA
$P_1^- = 50.30$ W	$P_1^0 = 59.72$ W	$S_{U1e} = 127.97$ VA
$TU_V = 16.91$ %		$TU_I = 62.32$ %
$THD_{V_e} = 1.90$ %		$THD_{V_{e1}} = 58.42$ %
$D_{eV} = 30.42$ VA	$D_{eI} = 935.38$ VA	$S_{eH} = 17.77$ VA
$D_{eH} = 15.25$ VA		$P_H = 9.12$ W

single-phase uncontrolled rectifier with an LC filter and a resistive load . The unbalanced linear load is connected from phase terminals to neutral wire and has the following values:

$$\begin{aligned} Z_{R \text{ load}} &= (R_{R \text{ load}} = 34 \Omega // L_{R \text{ load}} = 21 \text{ mH}); \\ Z_{S \text{ load}} &= (R_{S \text{ load}} = 57 \Omega // L_{S \text{ load}} = 12 \text{ mH}); \\ Z_{T \text{ load}} &= R_{T \text{ load}} = \infty \Omega. \end{aligned}$$

Table II displays the three-phase total harmonic distortion of the supplied current. Load fundamental currents are not equal, therefore even though non-linear loads need identical harmonic currents in all three phases, their quantities are not the same. Fundamental voltages from PCC line to neutral are measured at about 125 V and 80 V rms, respectively, throughout the testing. Using a three-phase Y-Y transformer with the phase terminal switched, the desired voltage asymmetry may be attained. Since the transformer's main is hardwired to the grid, the experimental testing account for 1.9% voltage distortion at the power conversion center (PCC). Before and after the SAPPCC is connected, there is little to no difference in the values of and the ratios and. The line-to-neutral voltage waveforms used in the testing are shown in

Fig. 9. All of the algorithms necessary for SACP control, such as SVPWM at a switching frequency equal to 19.2 kHz, dc bus voltage control, analog-to-digital conversion, current control, etc. [6], are implemented in a TMS320F2812 DSP. The circuit's primary magnitudes are shown in Tables III and IV, as they were in the preceding section. Voltages, currents, power levels, and the merit factor of the supply with the SACP turned off are all listed in Table III. Similar results may be seen in Table IV when the

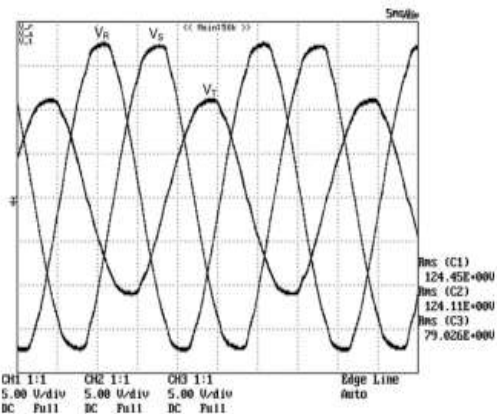


Fig. 5. Experimental phase-to-neutral supply voltage waveforms.

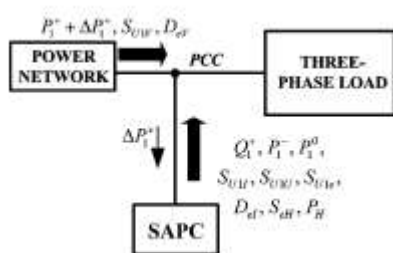


Fig. 6. Main power magnitudes when the SACP is connected.

The SACP link is active. The primary power magnitudes provided by the power network and the SACP are shown in Fig. 10. By using the SACP:

- is mitigated but not eliminated from the electrical grid. Both and are drastically lowered, while retaining the same value. Similarly, is decreased but not eliminated, and are mostly supplied by the SACP, while remaining connected to the electrical grid. The SACP's contributions to and represent the largest reductions. Since the SACP is unable to compensate for the PCC's voltage inequalities, we can only employ remains equal. The SACP operation modifies the new power words in a way that is analogous to the adjustment made to their corresponding terms in. and are close to zero as a result of the reduction. is quite close to 1, indicating that the system is functioning very close to optimally. The self-sustaining dc bus generates the marginal increase in. To make up for power losses in the SACP, the dc voltage controller

determines by how much the active power must increase [36, 38].

- The installation's power quality has improved, as measured by the values of the various power factors.

CONCLUSION

Electric power quantities that may exist in every state of an electric power network are defined in IEEE Std. 1459. In order to quantify energy and power in accordance with IEEE Std. 1459, a new generation of instruments is now in development. Unbalanced loads that use a SACP to correct for all unnecessary capabilities inspired more simulation and experimentation. The study introduces a new resolution of by using methods similar to those described in IEEE Std. 1459 for. The paper's calculations and experimental testing make advantage of the revised power magnitudes and factors. The obtained findings show that it is possible to differentiate between the various apparent powers in using the suggested resolution of. When SACP are used in customer installations to enhance power quality, the recommended power magnitudes provide for an explanation of the observed effects. Proper electrical energy billing and, in conjunction with other magnitudes, tracing the source of pollutions in imbalanced power networks are both made possible by the new power terms and factors.

REFERENCES

- [1] F. Blaabjerg, R. Teodorescu, M. Liserre, and A. V. Timbus, "Overview of control and grid synchronization for distributed power generation systems," *IEEE Trans. Ind. Electron.*, vol. 53, no. 5, pp. 1398–1409, Oct. 2006.
- [2] A. Arulampalam, M. Barnes, A. Engler, A. Goodwin, and N. Jenkins, "Control of power electronic interfaces in distributed generation microgrids," *Int. J. Electron.*, vol. 91, no. 9, pp. 503–523, Sep. 2004.
- [3] G. Hadjee and D. Sadarnac, "Coordination of residential load control for reducing system peak in rural electric power distribution," in *Proc. 5th IASTED Int. Conf. Power and Energy Systems*, Jun. 15–17, 2005, pp. 474–479.
- [4] L. S. Czarnecki, *Energy Flow and Power Phenomena in Electrical Circuits: Illusions and Reality*. New York: Springer-Verlag Electrical Engineering 82, 2000, pp. 119–126.
- [5] H. Akagi, E. H. Watanabe, and M. Aredes, *Instantaneous Power Theory and Applications to Power Conditioning*. Hoboken, NJ: Wiley, 2007.
- [6] S. Orts, F. J. Gimeno-Sales, A. Abellán, S. Seguí-Chilet, M. Alcañiz, and R. Masot, "Achieving maximum efficiency in three-phase systems with a shunt active power compensator based on IEEE Std. 1459," *IEEE Trans. Power Del.*, vol. 23, no. 2, pp. 812–822, Apr. 2008.
- [7] G. Escobar, A. A. Valdez, R. E. Torres-Olguin, and M. F. Martínez-Montejano, "A model-based controller for a three-phase four-wire shunt active filter with compensation of the neutral line current," *IEEE Trans. Power Electron.*, vol. 22, no. 6, pp. 2261–2270, Nov. 2007.

- [8] P. Rodriguez, A. V. Timbus, R. Teodorescu, M. Liserre, and F. Blaabjerg, "Flexible active power control of distributed power generation systems during grid faults," *IEEE Trans. Ind. Electron.*, vol. 54, no. 5, pp. 2583–2592, Oct. 2007.
- [9] H. Fujita and H. Akagi, "Voltage-regulation performance of a shunt active filter intended for installation on a power distribution system," *IEEE Trans. Power Electron.*, vol. 22, no. 3, pp. 1046–1053, May 2007.
- [10] D. O. Abdeslam, P. Wira, J. Mercklé, D. Flieller, and Y. Chapuis, "A unified artificial neural network architecture for active power filters," *IEEE Trans. Ind. Electron.*, vol. 54, no. 1, pp. 61–76, Feb. 2007.
- [11] C. Lascu, L. Asiminoaei, I. Boldea, and F. Blaabjerg, "High performance current controller for selective harmonic compensation in active power filters," *IEEE Trans. Power Electron.*, vol. 22, no. 5, pp. 1826–1835, Sep. 2007.
- [12] M. I. Montero, E. R. Cadaval, and F. B. Gonzalez, "Comparison of control strategies for shunt active power filters in three-phase four-wire systems," *IEEE Trans. Power Electron.*, vol. 22, no. 1, pp. 229–236, Jan. 2007.
- [13] J. Rodriguez, J. Pontt, C. A. Silva, P. Correa, P. Lezana, P. Cortes, and U. Ammann, "Predictive current control of a voltage source inverter," *IEEE Trans. Ind. Electron.*, vol. 54, no. 1, pp. 495–503, Feb. 2007.
- [14] S. Segui-Chilet, F. J. Gimeno-Sales, S. Orts, G. Garcerá, E. Figueres, M. Alcañiz, and R. Masot, "Approach to unbalance power active compensation under linear load unbalances and fundamental voltage asymmetries," *Int. J. Elect. Power Energy Syst.*, pp. 526–539, Sep. 2007.
- [15] S. Pajic and A. E. Emanuel, "Modern apparent power definitions: Theoretical versus practical approach-the general case," *IEEE Trans. Power Del.*, vol. 21, no. 4, pp. 1787–1792, Oct. 2006.
- [16] IEEE Trial Use Standard Definitions for the Measurement of Electric Power Quantities under Sinusoidal, Non-Sinusoidal, Balanced, or Unbalanced Conditions. *IEEE 1459–2000. Ins. of Electrical and Electronics Engineers, IEEE 1459–2000, 1, 2000.*
- [17] T. Zheng, E. B. Makram, and A. A. Girgis, "Evaluating power system unbalance in the presence of harmonic distortion," *IEEE Trans. Power Del.*, vol. 18, no. 2, pp. 393–397, Apr. 2003.
- [18] A. Ferrero, A. Menchetti, and R. Sasdelli, "Measurement of the electric power quality and related problems," *Eur. Trans. Elect. Power*, vol. 6, no. 6, pp. 401–405, Nov./Dec. 1996.
- [19] N. Locci, C. Muscas, and S. Sulis, "On the measurement of powerquality indexes for harmonic distortion in the presence of capacitors," *IEEE Trans. Instrum. Meas.*, vol. 56, no. 5, pp. 1871–1876, Oct. 2007.
- [20] C. Muscas, L. Peretto, S. Sulis, and R. Tinarelli, "Investigation on multipoint measurement techniques for PQ monitoring," *IEEE Trans. Instrum. Meas.*, vol. 55, no. 5, pp. 1684–1690, Oct. 2006.
- [21] P. V. Barbaro, A. Cataliotti, V. Cosentino, and S. Nuccio, "A novel approach based on nonactive power for the identification of disturbing loads in power systems," *IEEE Trans. Power Del.*, vol. 22, no. 3, pp. 1782–1789, Jul. 2007.
- [22] R. Arseneau, "Harmonic cost allocation with existing and proposed revenue metering methods," in *Proc. IEEE Power Eng. Soc. Summer Meeting*, Jul. 18–22, 1999, vol. 1, pp. 341–346.
- [23] R. Arseneau, "Application of IEEE standard 1459–2000 for revenue meters," in *Proc. IEEE Power Eng. Soc. General Meeting*, Jul. 13–17, 2003, vol. 1, pp. 87–91.
- [24] M. B. Hughes, "Electric power measurements—A utility's perspective," in *Proc. IEEE Power Eng. Soc. Summer Meeting*, Jul. 25, 2002, vol. 3, pp. 1680–1681.
- [25] A. E. Emanuel, "Summary of IEEE standard 1459: Definitions for measurement of electric power quantities under sinusoidal, nonsinusoidal, balanced, or unbalanced conditions," *IEEE Trans. Ind. Appl.*, vol. 40, no. 3, pp. 869–876, May/June 2004.